Solvent Induced Photophysics and Photochemistry of the (2p3s) Rydberg State of Diazabicyclooctane: Intersystem Crossing, Electron Transfer, and Energy Transfer

Q. Y. Shang,‡ P. O. Moreno,† and E. R. Bernstein*

Contribution from the Department of Chemistry, Colorado State University, Fort Collins, Colorado 80523

Received April 16, 1993. Revised Manuscript Received July 23, 1993®

Abstract: Solvent induced singlet (2p3s) Rydberg state relaxation dynamics of diazabicyclooctane (DABCO) are studied in van der Waals clusters generated in a supersonic jet expansion. The excited-state decay is determined by a pump (excitation)/probe (ionization) mass selective technique. Solvents employed for these cluster studies include rare gases, saturated hydrocarbons and fluorocarbons, amines, ethers, methyl sulfide, acetonitrile, and aromatics. The nature of the intermediate states to which the nascent singlet (2p3s) Rydberg state decays is determined based on excited-state lifetimes, cluster dissociation products, and ionization energies. At least three solvent induced relaxation pathways can be identified for the nascent DABCO Rydberg state: (1) intersystem crossing to the triplet (2p3s) Rydberg state, (2) internal conversion to an intermolecular charge-transfer state, and (3) energy transfer to an excited valence state of the solvent molecule. The (2p3s) triplet state origin is determined to lie at 564 cm^{-1} below the singlet state origin. The DABCO intersystem crossing rate is small but it can be significantly enhanced by the solvent molecule. Intermolecular electron transfer occurs in DABCO/amine, ether, and acetonitrile clusters. The electron-transfer state is determined to lie at least 650 cm^{-1} below the (2p3s) singlet Rydberg state. Energy transfer occurs in DABCO/aromatic clusters. The (2p3s) singlet Rydberg state dynamics are found to depend upon cluster geometry, cluster size, and cluster vibrational energy. These results suggest that the (2p3s) Rydberg state is reactive and susceptible to environmental perturbation.

I. Introduction

The relaxation dynamics of Rydberg states of amines in solution and gas phase are both rich and varied.[1-5] Many relaxation pathways have been proposed to account for the observed loss of fluorescence upon solvation and collision. The absence of fluorescence from amines solvated by or colliding with acetonitrile, perfluorocarbons, or sulfur hexafluoride is thought to be due to electron transfer from the excited-state amine to the ground-state solvent.[2-4] Sensitized emission is observed for dimethylethylamine in hexane solutions containing benzene or acetone, suggesting an energy-transfer mechanism for the deactivation of the amine Rydberg state.[5,6] Additionally, phosphorescence has been observed for diazabicyclo[2.2.2]octane (DABCO) in cold hexane matrices,[7] indicating relaxation of the Rydberg state to a triplet state through intersystem crossing. For many amines,[8-10] excimer formation is responsible for the quenching of the Rydberg state fluorescence. All of these observed relaxation pathways suggest that the amine Rydberg state is strongly influenced by its environment and thus susceptible to a number of solvent perturbations and reactions.

Rydberg orbitals are diffuse, of large spatial extent, and electrons in such orbitals are weakly bound. One would expect molecules in Rydberg states to be reactive, especially in the presence of solvent perturbations. Nonetheless, the study of the photophysical and photochemical behavior of Rydberg states has been quite limited.[11] An unambiguous assignment of the possible relaxation pathways and intermediate states for Rydberg state dynamics has not been forthcoming. Most previous studies of Rydberg state relaxation dynamics have been for amines. Amines possess a number of unique properties that make such studies both accessible and interesting: (1) the first excited state of saturated amines is the (2p3s) Rydberg state—thus no complications arise from Rydberg/valence state couplings as found for carbonyls, aromatics, and others;[11] (2) tertiary amines are typically photochemically stable;[11,12] and (3) Rydberg transition energies for many amines lie below 4 5 000 cm^{-1}. The understanding of amine Rydberg state behavior can contribute to the elucidation of the properties of systems as diverse as biological molecules and energetic materials.[13]

In three previous papers,[14-16] we have reported the study of static solvation effects on the (2p3s) Rydberg state of DABCO clustered with a wide variety of polar and nonpolar solvents. Many van der Waals clusters of DABCO have been observed spectroscopically; the (2p3s) ← $(2p)^2$ transition origins, van der Waals vibrations, internal vibrations, and cluster geometries have been assigned in the spectra. Three strong (2p3s) state/solvent interactions have been characterized for these clusters: repulsion, electron transfer or delocalization, and dipole/induced dipole. These interactions are manifested as large bare molecules to cluster shifts of the transition origins, both to lower and higher energies.

‡ Current address: Applied Materials, Santa Clara, CA.
† Current address: Dow Chemical Company, Freeport, TX.
* Abstract published in *Advance ACS Abstracts*, December 1, 1993.

(1) Halpern, A. M. *J. Phys. Chem.* **1981**, *85*, 1682.
(2) Halpern, A. M.; Taaghol, A. *J. Chem. Phys.* **1989**, *93*, 144.
(3) Halpern, A. M.; Forsyth, D. A.; Nosowitz, M. *J. Phys. Chem.* **1986**, *90*, 2677.
(4) Alford, P. C.; Cureton, C. G.; Lampert, R. A., Phillips, D. *Chem. Phys. Lett.* **1978**, *55*, 100.
(5) Halpern, A. M.; Wryzykowska, K. *Chem. Phys. Lett.* **1981**, *77*, 82.
(6) Halpern, A. M.; Wryzykowska, K. *J. Photochem.* **1981**, *15*, 147.
(7) Muto, Y.; Nakato, Y.; Tsubomura, H. *Chem. Phys. Lett.* **1971**, *9*, 597.
(8) Halpern, A. M.; Chan, P. P. *J. Am. Chem. Soc.* **1975**, *97*, 2971.
(9) Ramachandran, B. R.; Halpern, A. M. *J. Photochem. Photobiol. A: Chem.* **1991**, *58*, 1.
(10) Halpern, A. M.; Gerrity, D. P.; Rothberg, L. J.; Vaida, V. *J. Chem. Phys.* **1982**, *76*, 102.
(11) Robin, M. B. *Higher Excited States of Polyatomic Molecules*; Academic: New York, 1974; Vols. I, II, III.
(12) Nakajima, A.; Fuke, K.; Tsukamoto, K.; Yoshida, Y.; Kaya, K. *J. Phys. Chem.* **1991**, *95*, 571.
(13) Olah, G. A.; Squire, D. R. *Chemistry of Energetic Materials*; Academic: New York, 1991.
(14) Shang, Q. Y.; Moreno, P. O.; Li, S.; Bernstein, E. R. *J. Chem. Phys.* **1993**, *98*, 1876.
(15) Shang, Q. Y.; Moreno, P. O.; Dion, C.; Bernstein, E. R. *J. Chem. Phys.* **1993**, *98*, 6769.
(16) Shang, Q. Y.; Moreno, P. O.; Bernstein, E. R. *J. Am. Chem. Soc.*, preceding paper in this issue.

0002-7863/94/1516-0311$04.50/0

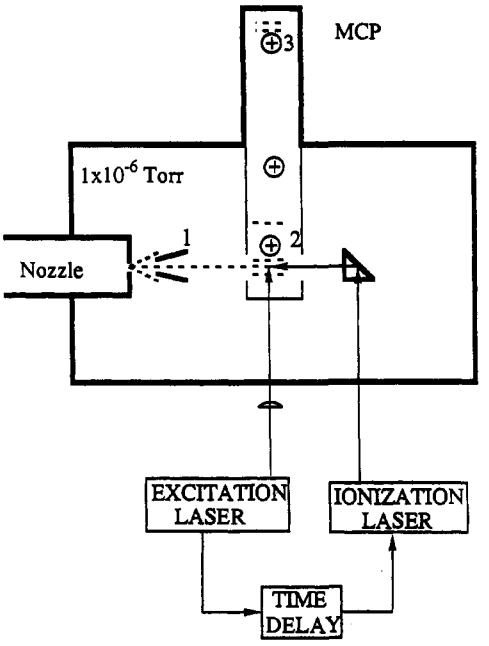

Figure 1. Experimental schematic for the pump/probe supersonic jet technique. The lasers are Nd/YAG pumped dye lasers. Pulse triggering and delays for the two lasers are controlled by an external delay generator. The different parts of the apparatus are (1) skimmer, (2) high voltage grids, and (3) multichannel plate detector.

In this report, we address solvent induced relaxation dynamics of the (2p3s) excited Rydberg state of DABCO/solvent van der Waals clusters. The systems are created, cooled, and isolated in a supersonic jet expansion. The relaxation processes identified for these clusters depend sensitively on solvent, cluster geometry, cluster size, and cluster vibrational energy in the Rydberg electronic state. The intermediate states to which the nascent Rydberg state relaxes are determined from cluster decay curves, ionization thresholds, and dissociation products. Depending on the solvent molecule, the intermediate states that arise from the singlet Rydberg state include the Rydberg (2p3s) triplet state, an electron-transfer state, or an excited state of the solvent reached through energy transfer. The reasons for this varied relaxation behavior are discussed.

II. Experimental Procedures

A. Pump/Probe Technique. Our supersonic jet expansion apparatus and mass resolved excitation spectrometer have been previously described in the literature.[17] A pump/probe ionization technique is used to measure the population decay of both the bare molecule and clusters. A schematic diagram of the experiment is presented in Figure 1. The excitation laser is described in a previous paper.[16] The excitation laser beam is mildly focused with a 1-m focal length lens that is placed ca. 70 cm from the molecule beam ionization region. This focusing is designed to create a large excited state population while reducing the spatial distribution of excited species. The ionization laser is a Nd/YAG third harmonic pumped dye laser with wavelength coverage from 430 to 520 nm (using dyes C440, C460, C480, and C500-Exciton Corp.). The energy output of this laser is 15–20 mJ/pulse in a beam diameter of 0.4 cm. The excitation laser power is reduced so that the one-color signal is small, while the two-color signal is intense (typically a 1/10 one-color/two-color signal ratio). The laser triggering and time delay are achieved by an SRS time delay pulse generator. A perpendicular pump/probe configuration is employed with the probe beam counter propagating with respect to the molecular beam on the beam axis. This geometry ensures that the signal is available over the full lifetime of the nascent excited state. In this geometry the detection time limit is governed by the aperture of the time of flight mass spectrometer and thus the voltage grid size: the grid is ca. 1-cm in diameter, and the beam velocity is ca. 2×10^5 cm/s. These estimates predict a 5.0 μs observation time which is close to the 3.5 μs actual upper limit to the apparatus measurement time.

(17) Bernstein, E. R.; Law, K.; Schauer, M. *J. Chem. Phys.* **1984**, *80*, 207.

Scheme I

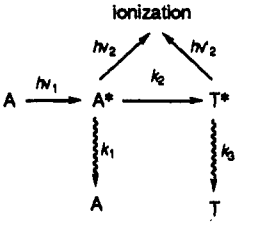

The excited-state population decay of the DABCO molecule or cluster is measured by the loss in signal from the particular mass channel of interest. This technique has the advantage that dark states that have reasonable lifetimes can be accessed.

This same experimental configuration is employed to measure ionization thresholds for the excited-state species at fixed excitation energies and at particular time delays. A delayed threshold ionization measurement can determine the threshold for the intermediate state generated by decay of the nascent state.

B. Analysis of the Pump/Probe Decay Data. The possible excited-state relaxation pathways are presented in Scheme I. This kinetic scheme assumes the existence of an intermediate excited state T^* to which the nascent state A^* relaxes. The total ion intensity can be expressed as a function of time:

$$I(t) = A\exp[-(k_1 + k_2)t] + B\exp[-k_3 t] \quad (1)$$

in which A and B are constants related to the k_is and the initial concentration of A^*, k_1 is the radiative decay rate for A^*, k_2 is the relaxation rate of A^* to T^*, k_3 is the total decay rate of T^*, and t is the time delay between the pump and probe laser pulses. If τ is the lifetime of A^*, and τ_3 is the lifetime of T^*, then

$$\tau = 1/(k_1 + k_2) \quad (2)$$

and

$$\tau_3 = 1/k_3 \quad (3)$$

When k_2 is zero, B is zero, and the decay of A^* can be represented by a single exponential function: the only loss of A^* comes from fluorescence (radiative lifetime). When τ_3 is large, eq 1 can be written as

$$I = A\exp[-t/\tau] + B \quad (4)$$

Equation 4 is used to fit the signal intensity for an initial fast decay to a constant signal intensity. Triplet states typically have lifetimes many orders of magnitude longer than their comparable singlet states.

Depending on the shape of the experimental decay curve, eq 1, eq 4, or a single exponential can be used to fit the decay curve. The instrument response function is ca. 10 ns and, for decays in excess of 100 ns, it is omitted from the fitting procedure. The reported lifetimes have an uncertainty of about 10%.

III. Results

A. Bare Molecule. Figure 2 shows the pump/probe decay curve of the (2p3s) excited singlet Rydberg state ($^1R_1$) of isolated cold DABCO. The excitation at 36 236 cm^{-1} pumps the first observed one-photon allowed vibronic transition, 450 cm^{-1} above the bare molecule two-photon allowed origin (0_0^0, 35 786 cm^{-1}): the 0_0^0 feature of this transition is one-photon forbidden.[14] The ionization laser energy is at 22 222 cm^{-1}, close to the ionization threshold of the (2p3s) singlet state (see below). The abrupt decrease in signal intensity at ca. 3.5 μs gives the limits of long time measurements by the pump/probe technique employed here. In 3.5 μs the molecules have traveled roughly 7 mm. The data are only fit to ca. 3.5 μs. The lifetime extracted from this single exponential decay is 1.8 μs. The decay curve for a vibration at 0_0^0 + 691 cm^{-1} is also measured. The lifetime fit to this curve is ca. 1.7 μs.

The displayed decay curve in Figure 2 contains a 0.3 μs periodic modulation even after averaging 10 different decays (a total of 100 laser pulses/point on the curve). The cause of this modulation has not been determined. The only other species in this study

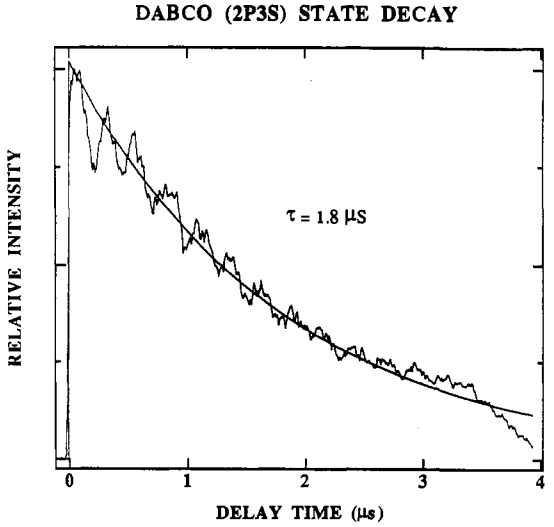

Figure 2. Pump/probe decay curve of the DABCO bare molecule at its first one-photon allowed vibronic transition at 36 236 cm^{-1}. Ionization laser energy is 22 300 cm^{-1}. The solid smooth curve represents a fit of the decay curve to a single exponential function with a 1.8 μs lifetime. The abrupt decrease of the signal after 3.5 μs is due to the instrumental detection limit.

Table I. The Singlet (2p3s) Excited-State Lifetimes of DABCO and Its Solvent Clusters Obtained from Pump/Probe Ionization Measurements[c]

DABCO (solvent)$_1$	excitation (cm^{-1})	lifetime (μs)	IP $^1R_1$[a] (cm^{-1})	assignments/ comments
bare DABCO	36 236	1.8		$0_0^0 + 450$[b]
Ar	35 891	1.7	22 136	origin I
	36 088	1.4	21 870	broad, origin II
Kr	35 882	1.3		origin I
	36 075	0.4	21 910	broad, origin II
CH_4	35 935	1.25	21 860	origin I
CF_4	36 206	1.3	21 755	origin I
	36 640	0.85		origin II
C_2F_6	36 090	0.91		origin
methylcyclohexane	36 181	1.4		origin
benzene	35 452	0.17	20 900	origin
toluene	35 422	0.15		origin
CH_3SCH_3	35 858	0.33		origin
dioxane	35 700	0.40		broad
CH_3OCH_3	35 327	0.25	19 963	origin I
	35 451	0.32		origin II
THP	35 233	0.26		origin I
	35 511	0.90		origin II
DABCO	35 245	0.2		origin
TEA	35 364	0.28	19 920	origin I
	35 562	0.38		origin II
NH_3	35 650	0.19		broad
CH_3CN	35 650	0.10		broad

[a] IP $^1R_1$ is the ionization threshold energy of the $^1R_1$ state excited. [b] First one-photon allowed vibronic feature. Lifetime of this feature and others of bare molecule DABCO are the same. [c] Excitation is always at the assigned origins of the respective clusters.

that shows similar effects is the DABCO dimer (see below). Possible coherences that might develop at this degree of excitation and for this beat or modulation frequency would be between the (2p3s) Rydberg singlet ($^1R_1$) state and triplet ($^3R_1$) state.

B. DABCO/Rare Gas and Saturated Hydrocarbon Clusters. Decays of the DABCO/rare gas and saturated hydrocarbon clusters excited $^1R_1$ 0^0 states are measured and presented in Table I. These studies are designed to parallel those for the bare molecule, and thus the ionization laser energy for these measurements is maintained at 22 222 cm^{-1}. In previous papers (refs 14, 25, and 16) we identify clusters of the same mass that possess different cluster geometries. In particular, for DABCO (rare gas)$_n$ clusters solvation sites at the methylene bridges and the nitrogen atoms are identified.[14,15] When multiple geometries are

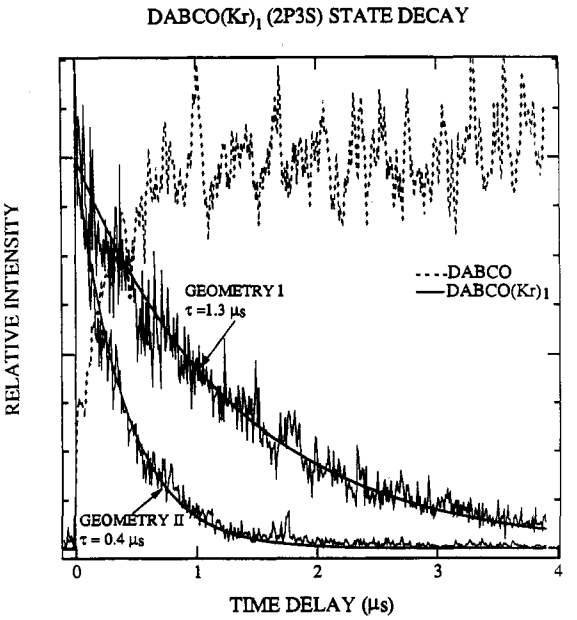

Figure 3. Decay (solid curve) of DABCO(Kr)$_1$ ion signal and rise (dashed curve) of the DABCO bare molecule ion signal. Excitation at 35 882 cm^{-1} pumps the DABCO(Kr)$_1$ "geometry I" cluster with Kr located between two C–C bridge ethylenes of DABCO and excitation at 36 075 cm^{-1} pumps the DABCO(Kr)$_1$ "geometry II" cluster with Kr located at the nitrogen end of DABCO. The ionization laser energy is 22 222 cm^{-1}. Note that the cluster signal decays can be fit to a single exponential function and that the signal approaches zero at later time. The bare molecule signal (dashed curve) is obtained when the cluster geometry II origin is pumped and ionized at 23 076 cm^{-1}. The signal has a initial rise of $\tau \approx 0.4$ μs and then remains constant (see text for interpretation).

identified for a given cluster composition, decays for both geometries are measured. The decays for all these clusters can be fit to a single exponential function. An example of such behavior is presented in Figure 3 for DABCO(Kr)$_1$.

As can be seen in Table I, DABCO/rare gas and saturated hydrocarbon clusters in the $^1R_1$ state show a reduced lifetime compared to that of the bare DABCO molecule. For DABCO-(Ar)$_1$, the lifetimes for two geometries are 1.7 and 1.4 μs, respectively. For DABCO(Kr)$_1$ the lifetimes further decrease to 1.3 and 0.4 μs for the corresponding two geometries. These geometries are identified as discussed in the preceding paper and in refs 14 and 15. In both cases the lifetime is much shorter for the cluster with solvent located nearer the nitrogen atom.[14,16] The decrease of the lifetime could be due either to an increased radiative rate or to solvent assisted nonradiative relaxation. The following results will demonstrate that this reduced lifetime for the cluster $^1R_1$ 0^0 state is primarily due to solvent induced intersystem crossing to the DABCO $^3R_1$ Rydberg state.

Also shown in Figure 3 is the rise time of a signal in the bare molecule DABCO mass channel generated by $^1R_1$ $0^0 \leftarrow S_0$ excitation of the DABCO(Kr)$_1$ cluster with geometry II. This cluster geometry is identified in ref 16 as that with the rare gas atom coordinated to the nitrogen end of the DABCO molecule. This rise time coincides with the decay of the cluster signal. At long times ($\tau \gg 2$ μs) the signal in the bare molecule mass channel remains constant, while the DABCO(Kr)$_1$ signal decays to zero. These results show that the bare molecule signal arising from excitation of the cluster is not due to dissociation of the DABCO-(Kr)$_1$ cluster ion. The new signal in the bare molecule mass channel must arise from the neutral cluster excited to the $^1R_1$ 0^0 state. The kinetic scheme for this process is given below.

Figure 4 presents the ionization threshold energy for the DABCO bare molecule excited at $^1R_1$ $0^0 + 691$ cm^{-1} and for the DABCO species created by DABCO(Kr)$_1$ neutral cluster dissociation. The energy difference shows that the DABCO molecule

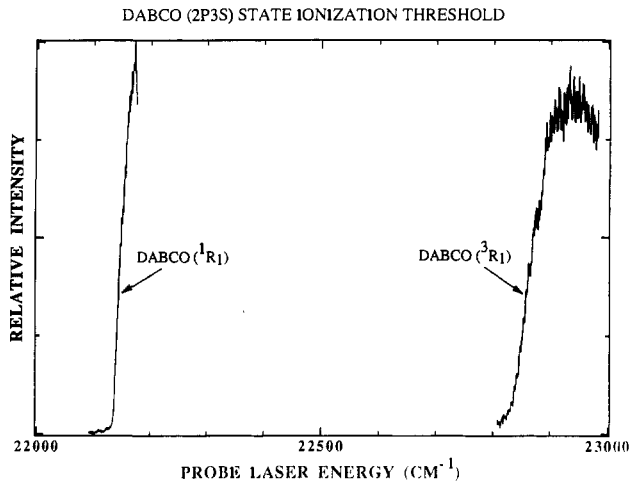

Figure 4. Photoionization threshold spectra of the excited singlet and triplet Rydberg states of DABCO. The singlet excited state ($^1R_1$) ionization curve is obtained by excitation of DABCO at its vibronic transition peak at 36 477 cm^{-1}. The triplet Rydberg state ($^3R_1$) ionization curve is obtained by excitation of the DABCO(Kr)$_1$ "geometry II" cluster transition at 36 075 cm^{-1}, while monitoring the DABCO ion mass channel with the ionization laser delayed 3 μs with respect to the excitation laser. The ionization energies for $^1R_1$ and $^3R_1$ states are 22 137 and 22 830 cm^{-1}, respectively.

generated through cluster dissociation is in a state lower in energy than the $^1R_1$ 0^0 state. Since the $^1R_1$ state is believed to be the lowest singlet state of DABCO,[18] this new state is most likely the $^3R_1$ state of DABCO. All the other clusters in this general category of clusters behave in a comparable fashion (see Table I).

The kinetic scheme that rpresents the overall behavior of these DABCO clusters is

$$\underset{S_0}{DABCO(X)_1} + h\nu \rightarrow \underset{^1R_1}{DABCO(X)_1} \xrightarrow{k_{ISC}}$$

$$\underset{^3R_1}{DABCO(X)_1} \xrightarrow{k_{IVR/VP}} \underset{^3R_1}{DABCO} + X$$

The intersystem crossing process generates a cluster that has vibrational energy given by $E(^1R_1\ 0^0) - E(^3R_1\ 0^0) = {}^{1,3}\Delta E$. If ${}^{1,3}\Delta E$ is greater than the cluster binding energy, the cluster rapidly undergoes intracluster vibrational energy redistribution (IVR) followed by vibrational predissociation (VP).[19] The observed newly created DABCO molecule has a very long lifetime as is expected for the lowest lying triplet state. The cluster lifetimes generally display a trend that is consistent with the heavy atom effect on intersystem crossing.

From the data presented in Figure 4 and the total ionization energy reported for DABCO (58 052 cm^{-1})[18] we can construct an energy level diagram for the DABCO molecule. The two-photon allowed $^1R_1$ 0_0^0 transition lies at 35 786 cm^{-1}, and thus the DABCO $^1R_1$ 0^0 state has an ionization threshold of 22 266 cm^{-1}. Thus the triplet state origin, requiring an ionization energy of 22 830 cm^{-1}, must lie 564 cm^{-1} below the singlet state origin. Additionally, the one-photon excitation at 0_0^0 + 691 cm^{-1} (36 477 cm^{-1}) has an ionization threshold of 22 137 cm^{-1}. Since ionization is most likely a $\Delta v = 0$ process, the 691-cm^{-1} mode in $^1R_1$ becomes 562 cm^{-1} in the ion. These results are summarized in Figure 5.

(18) Smith, M. A.; Hager, J. W.; and Wallace, S. C. *J. Phys. Chem.* **1984**, *88*, 2250.

(19) (a) Hineman, M. F.; Kim, S. K.; Bernstein, E. R.; Kelley, D. F. *J. Chem. Phys.* **1992**, *96*, 4904. (b) Hineman, M.; Bernstein, E. R.; Kelley, D. F. *J. Chem. Phys.* **1993**, *98*, 2516. (c) Nimlos, M. R.; Young, M. A.; Bernstein, E. R.; Kelley, D. F. *J. Chem. Phys.* **1989**, *91*, 5268 and references to earlier work cited therein. (d) Outhouse, E. A.; Bickel, G. A.; Dremmer, D. R.; Wallace, S. C. *J. Chem. Phys.* **1991**, *95*, 6261.

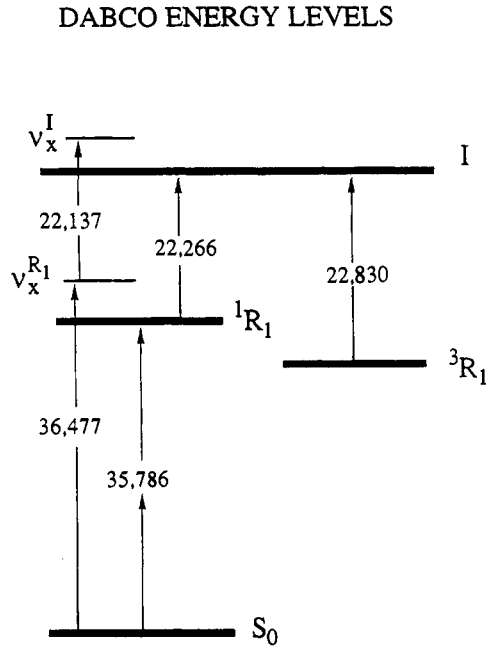

Figure 5. Experimentally determined energy level diagram of the DABCO bare molecule (cm^{-1}). The value for the $^1R_1$ 0^0 ionization energy is obtained from the reported total ionization energy (58 052 cm^{-1}) minus the excitation energy.

C. DABCO/Fluorocarbon Clusters. Figure 6 displays the experimental excited-state decay curves of DABCO$(CF_4)_1$ and $(C_2F_6)_1$ generated by excitation at their respective origins.[15] The decay curve for DABCO$(CF_4)_1$, like that for DABCO$(CH_4)_1$, can be fit to a single exponential decay function with a lifetime of 1.3 μs. Though very weak, a rise in the bare molecule mass channel signal intensity can be detected if the ionization probe laser has enough energy (greater than 22 830) cm^{-1}) to ionize the triplet state of the bare molecule. This suggests that the decreased lifetime of the $^1R_1$ 0^0 cluster state is due to a solvent enhanced intersystem crossing, as discussed above for DABCO/rare gas clusters.

Attempts were made to observe lifetimes of higher vibrational levels of these clusters in order to distinguish between various possible final states and vibrational predissociation in the $^1R_1$ state. Unfortunately, signals are too weak to obtain reliable relaxation data.

The DABCO$(C_2F_6)_1$ cluster decay curve for $^1R_1$ 0^0, however, cannot be fit to a single exponential decay function as shown in Figure 6. A much slower relaxation process seems to be important at longer times. The experimental decay can be fit by the function

$$I(t) = 0.91\ \exp(-t/0.91) + 0.09\ \exp(-t/154) \qquad (5)$$

The short time rate constant is $k_1 \sim (0.91\ \mu s)^{-1}$ and long time rate constant is $k_2 \sim (150\ \mu s)^{-1}$. No bare molecule signal is observed for this cluster with the probe laser energy sufficiently high for triplet state ionization to occur. Thus the binding energy of the cluster must be greater than ca. 600 cm^{-1} (see Table I and Figure 5). This amount of energy is roughly the van der Waals vibrational energy put into the triplet state of the cluster upon intersystem crossing and subsequent rapid vibration redistribution of energy.[19] While the triplet state has long lifetime, the cluster DABCO$(C_2F_6)_1$ shortens it considerably, probably through enhanced $^3R_1 \rightarrow S_0$ intersystem crossing.

D. DABCO/Amine, Ether, and Acetonitrile Clusters. 1. Excitation at Cluster Origin. Figures 7 and 8 display decay curves for the lowest energy cluster origins of DABCO$(NH_3)_1$, (triethylamine)$_1$ [(TEA)$_1$], (DABCO)$_1$, (dioxane)$_1$, $(CH_3OCH_3)_1$, and (tetrahydropyran)$_1$ [(THP)$_1$]. The ionization laser energy used in these cluster studies (22 222 cm^{-1}) is near the bare molecule

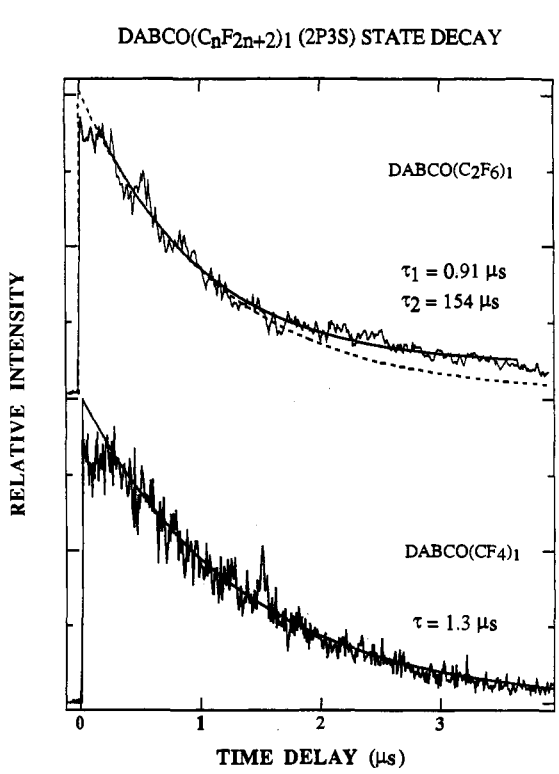

Figure 6. Decay of DABCO/perfluorocarbon cluster (2p3s) singlet Rydberg states. The ionization energy is 22 222 cm^{-1}. Both clusters are excited at their origin transitions (36 206 cm^{-1} for $(CF_4)_1$ and 36 090 cm^{-1} for $(C_2F_6)_1$ clusters). The DABCO$(CF_4)_1$ decay is fit to a single exponential function with a lifetime of 1.3 μs. The DABCO$(C_2F_6)_1$ decay curve is best fit by a biexponential decay function (solid line); a single exponential decay function (dashed line) generates a poor fit.

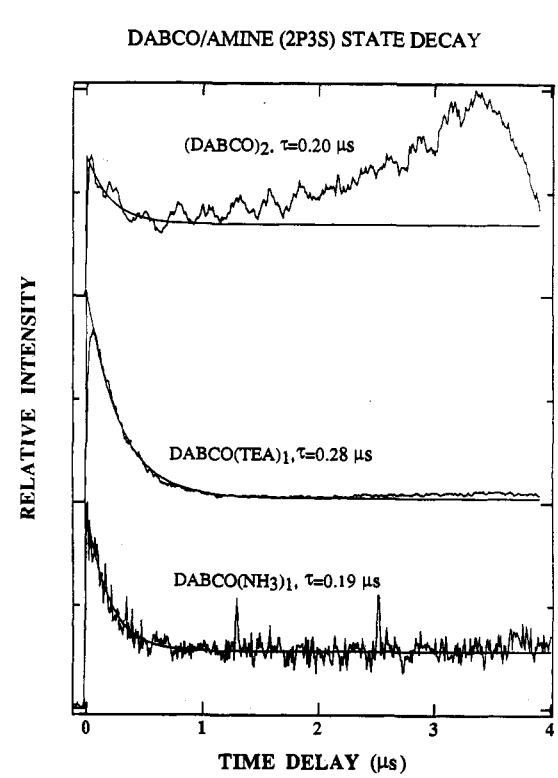

Figure 7. Decay of DABCO/amine cluster (2p3s) Rydberg state observed through origin excitation. The ionization energy is 22 222 cm^{-1}. Note that the decays end in a constant signal for each case. These curves have been fit to single exponential function plus a constant. The constant signal is assigned as due to long-lived charge-transfer intermediate. The signal rise at later time is probably due to solvent reorganization accompanied by an ionization efficiency enhancement.

ionization threshold in all instances. This energy is not sufficient to ionize the triplet state of DABCO. These decay curves are characterized by three observations: (1) a fast decay of the initially excited cluster $^1R_1$ state; (2) after roughly 1 μs the signal in the cluster mass channel is a nonzero constant; and (3) some increase in this constant signal is observed at long time, especially for $(DABCO)_2$. A similar decay curve is observed for DABCO-$(CH_3CN)_1$.

These curves are fit to the functional form given in eq 4 with the rise at ~3 μs ignored. The extracted lifetimes are given in Figures 7 and 8 and Table I. The lifetime for DABCO$(CH_3CN)_1$ is 0.1 μs. The results suggest that the excited cluster $^1R_1$ 0^0 relaxes to another state in less than 0.4 μs and that this new state is long lived.

The ionization thresholds for the initially excited $^1R_1$ 0^0 state of the cluster and the new state have been determined. The results are presented in Figure 9 for DABCO$(CH_3OCH_3)_1$ and $(TEA)_1$ clusters. The ionization energy of the initially excited state ($^1R_1$ 0^0) is obtained when the two lasers (pump and probe) are coincident in time. The ionization thresholds under these conditions are 19 963 cm^{-1} for DABCO$(CH_3OCH_3)_1$ and 19 920 cm^{-1} for DABCO$(TEA)_1$. The new state threshold is measured when the ionization laser is delayed with respect to the pump laser by at least 3 μs. As can be seen in Figure 9, the ionization threshold for these clusters is increased by roughly 650 cm^{-1} for this new state.

These decay curves are also measured with an ionization laser energy of 20 000 cm^{-1} for DABCO$(CH_3OCH_3)_1$ and $(TEA)_1$ excited at the cluster origin. This is not sufficient energy to ionize the triplet state of DABCO or these clusters: thus the new state cannot be ionized with 20 000 cm^{-1} of ionization laser energy. In this case the signal decay can be fit with a single exponential function without a constant term (i.e., $B = 0$ in eq 4). These measured lifetimes are similar to those obtained with 22 222 cm^{-1} probe ionization laser energy.

DABCO/ETHER (2P3S) STATE DECAY

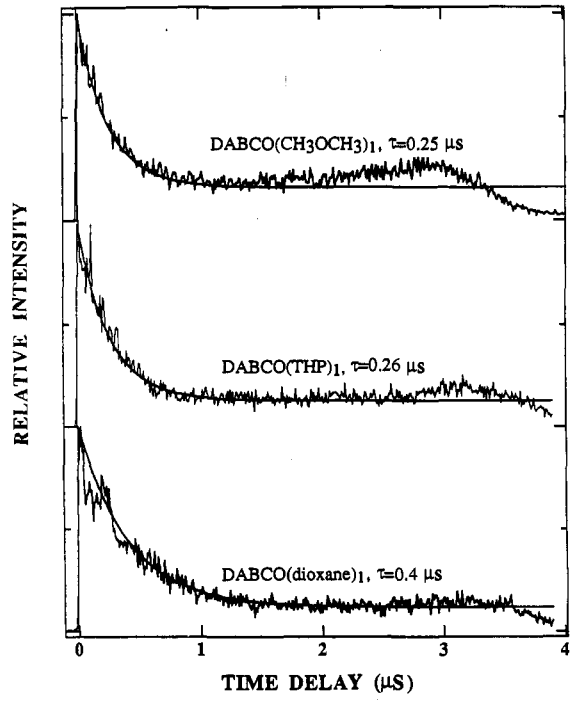

Figure 8. Decay of DABCO/ether cluster (2p3s) Rydberg state observed through origin excitation. The conditions and conclusions are the same as described for Figure 7.

In the next section we present experimental evidence to suggest that this new state is not a highly shifted triplet state of the DABCO/amine, ether, CH_3CN cluster system.

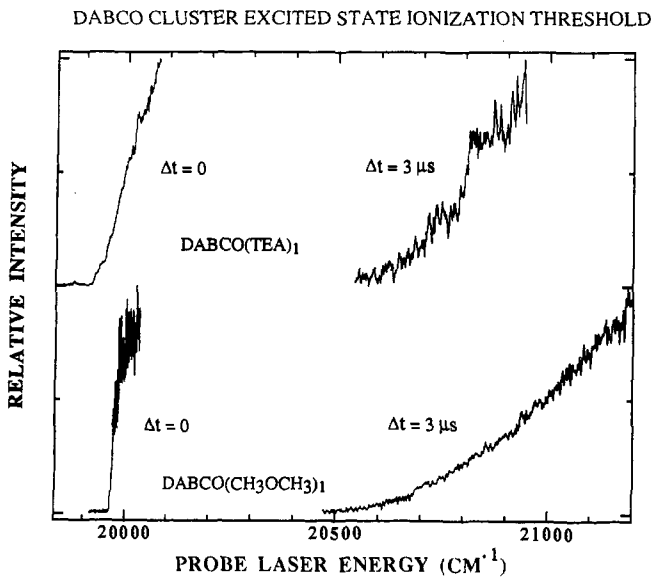

Figure 9. Photoionization threshold energy spectra for DABCO(CH_3OCH_3)$_1$ and DABCO(TEA)$_1$ (2p3s) Rydberg state. Excitation is at the cluster first observed origin transition. Δt represents the time delay between the excitation laser and the ionization laser.

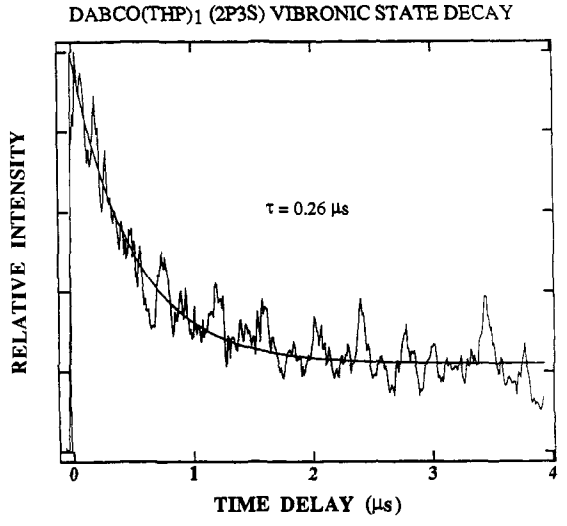

Figure 10. Decay of DABCO(THP)$_1$ excited at 36 898 cm^{-1} (0_0^0 + 1665 cm^{-1}). The ionization energy is 22 222 cm^{-1}. Note the signal does not approach zero at long times. The decay curve can be fit to a single exponential function plus a constant. This result indicates that the DABCO(THP)$_1$ cluster does not dissociate in the new state.

Finally, we suggest that the rise in the constant signal at long times (>3 μs) is caused by solvent/solute reorganization within the cluster which enhances the cross section for ionization as the cluster achieves its new equilibrium geometry.

2. Excitation at a Cluster Vibronic Transition. To determine the nature of the new excited state of DABCO/amine, ether, and CH_3CN clusters, we consider the ionization and vibrational predissociation of the clusters. The new excited state of these clusters does not dissociate as can be seen from the long lifetime constant signal in Figures 7 and 8. This observation might be explained by a large cluster binding energy for a newly created triplet state. The amount of vibrational energy gained by the cluster following $^1R_1 \rightarrow {}^3R_1$ intersystem crossing is roughly 560 cm^{-1} as established for DABCO(Kr)$_1$: the singlet–triplet separation should not in general be greatly perturbed by cluster formation and the binding energies for the two states $^1R_1$ and $^3R_1$ should be quite similar. From paper 1,[16] the experimental upper limit for the $^1R_1$ state dissociation energy for DABCO/amine, ether clusters, and (DABCO)$_2$ is about 1600 ± 100 cm^{-1}. Thus the 564 cm^{-1} gained from intersystem crossing will not dissociate these clusters upon $^1R_1\ 0^0 \rightarrow {}^3R_1\ X^n$. The binding energy for $^1R_1$ and $^3R_1$ should be quite comparable for these clusters.

The decay curves are then measured for these clusters with increased vibrational energy in the (2p3s) singlet Rydberg state. A typical example is shown for DABCO(THP)$_1$ in Figure 10. The excitation laser for this experiment is set at $^1R_1\ 0^0$ + 1665 cm^{-1}, 36 898 cm^{-1}. The decay curve is similar to the one obtained for excitation at $^1R_1\ 0^0$: a fast decay plus a constant signal. The constant signal level after 1 μs must be due to the new state formation. The new state now has at least 2270 cm^{-1} of excess vibrational energy. This would certainly be sufficient energy to dissociate the $^3R_1$ cluster state. Since the cluster does not dissociate at long times, we assume the new state is not the triplet state. The new state is assigned as charge- or electron-transfer state between DABCO and its amine, ether, or CH_3CN solvent. This state will be further discussed in the Discussion section.

The bare DABCO molecule mass channel signal is also monitored during this latter experiment. A curve similar to the dotted one in Figure 3 is observed when the ionization energy is above the bare molecule triplet ionization energy threshold (22 830 cm^{-1}). The signal level in the bare molecule mass channel is about five times weaker than that in the cluster mass channel. No rise is observed in the bare molecule mass channel if the cluster is excited at $^1R_1\ 0^0$. This suggests that $^3R_1$ DABCO(THP)$_1$ is also formed and does dissociate at 2270 cm^{-1} of vibrational energy but that it is a minor product. DABCO/amine clusters display the same behavior. An overall mechanism that is consistent with these observations is presented in Scheme II.

Scheme II. Electron Transfer and Triplet State Cluster Population

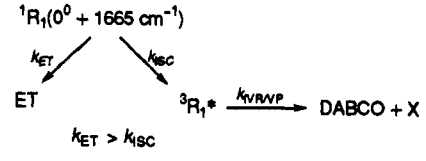

3. Relaxation and Cluster Geometry. As previously pointed out, DABCO(THP)$_1$, (TEA)$_1$, and (CH_3OCH_3)$_1$ cluster spectra arise from more than one cluster geometry. The $^1R_1\ 0^0$ decay rate for each observed geometry is measured. The fitted lifetimes of these clusters are compiled in Table II. All geometries show the behavior described in Scheme II. The cluster geometry with the most red shifted transition origin has the shorter lifetime; that cluster has been previously assigned as the one for which the solvent is located at the nitrogen atom end of the DABCO molecule.[14-16]

4. Relaxation Dependence on Vibrational Excitation. The decay rate of different internal DABCO vibrations is also studied. The results are listed in Table II. The general trend in lifetimes seems to be that the origin has the fastest decay and higher vibrational levels of DABCO in amine and ether clusters relax more slowly. While this trend seems somewhat counterintuitive, the separations between $^1R_1$, $^3R_1$, and the electron-transfer state are small enough that specific resonances between them and specific Franck–Condon factors for the processes can play an important role in the observed decays.

5. Cluster Size Effects. The effect of cluster size on the relaxation rates can also be measured. The relaxation rates at the (2p3s) singlet Rydberg origin are presented in Table III for DABCO(NH_3)$_n$, n = 1, 2, 3, and DABCO(CH_3OCH_3)$_n$, n = 1, ..., 5. These amine and ether clusters show the same general behavior as previously described. The decay curves show a rapid fall at short times which tends toward a constant value at long times (see Figures 6, 7, and 9). The decay for the amine clusters (Table III) is relatively constant with increasing cluster size.

Table II. Comparison of the Singlet (2p3s) Excited-State Lifetimes of DABCO/Amine and Ether Clusters with Different Internal and External Vibrational Excitations[b]

cluster and assignment[a]	excitation (cm^{-1})	lifetime (μs)
	DABCO(THP)$_1$	
origin I	35 233	0.26
vdW, c (57)	35 290	0.22
iv, C (780)	36 013	0.50
iv, D (890)	36 123	0.50
iv, E (1272)	36 505	0.42
iv, 2 × C (1573)	36 806	0.35
iv, C + D (1665)	36 898	0.50
	DABCO(TEA)$_1$	
origin I	35 364	0.28
iv, C (778)	36 142	0.38
	DABCO(CH_3OCH_3)$_1$	
origin I	35 327	0.25
iv, C (782)	36 109	0.28

[a] vdW stands for intermolecular van der Waals vibration and iv stands for internal vibration of DABCO. See ref 16 for assignments. [b] The ionization energy is 22 222 cm^{-1}.

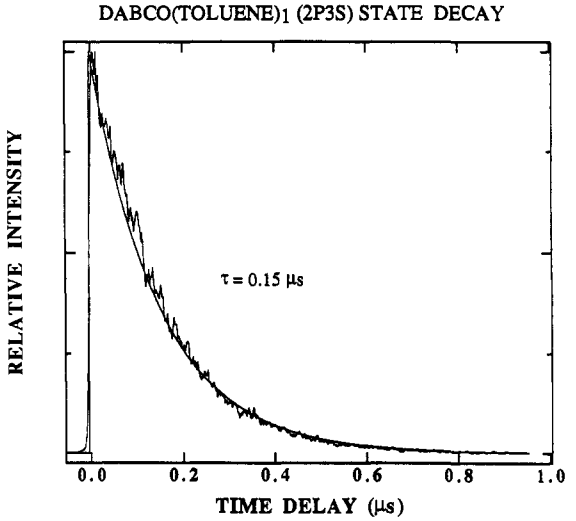

Figure 11. Decay of the DABCO(toluene)$_1$ excited state measured for transition origin excitation. The ionization energy is 22 222 cm^{-1}. The data show a fast single exponential decay to zero signal. This decay is assigned as due to DABCO to toluene energy transfer.

The lifetime of the DABCO(CH_3OCH_3)$_1$ $^1R_1$ 0^0 state is ca. 0.25 μs. In this case the $n = 2$ cluster has a very short lifetime and the larger clusters show lifetimes about one-half that of the $n = 1$ cluster. Cluster fragmentation should not be a serious concern for these systems as threshold ionization is achieved in all instances.

E. DABCO/Aromatic and CH_3SCH_3 Clusters. The DABCO-(toluene)$_1$ decay curve is presented in Figure 11, and the lifetime is tabulated in Table I. The decay is rapid and can be fit to a single exponential. These signals decay to zero and no signal with a comparable rise time can be found in the bare molecule mass channel. The same decay behavior is found for ionization laser energy 22 222 or 28 170 cm^{-1}. This latter energy is clearly sufficient to ionize either an electron transfer state of the cluster or a triplet state of DABCO. As can be seen from Table I, fast decay rates are also found for DABCO(benzene)$_1$ and (CH_3-SCH_3)$_1$. All three of these clusters behave in a similar manner: no longtime, constant signal in the decay and no cluster fragmentation into the bare molecule mass channel.

The decays observed for these clusters cannot be associated with intersystem crossing or electron transfer. Yet the short lifetimes and single exponential decay behavior suggest some additional relaxation mechanism is dominant here. In the Discussion section we argue that the relaxation mechanism involves energy transfer to an aromatic valence state.

IV. Discussion

The fluorescence quantum yield for DABCO is reported to be near unity in a collisionless regime.[20] Thus, the decay of excited state DABCO is dominated by radiative processes. The reported gas-phase lifetime is 1.04 μs,[20] which is significantly shorter than the 1.8 μs lifetime observed in this work for supersonic expansion cooled DABCO. This discrepancy could be due to excitation of room temperature DABCO (broad spectrum) to other (2p3s) or (2p3p) Rydberg states which subsequently relax to the lowest (2p3s) Rydberg with large vibrational excitation. Internal conversion thousands of cm^{-1} above the $^1R_1$ 0^0 state (at the absorption Franck–Condon maximum) could be faster than at the origin.

Extensive work has appeared for (2p3s) Rydberg state relaxation dynamics of amines in solution.[1-5] Solution fluorescence is characterized by reduced quantum yields and often multiexponential decays. The various relaxation pathways suggested to explain the solution fluorescence data differ for different amines and different solvents.[1-5] In many instances, however, excimer or exciplex formation has been suggested as the relaxation intermediate. These intermediate "states" are characterized by low quantum yields for fluorescence and long lifetimes. The relaxation behavior observed in this work shows that many channels for relaxation and even reaction are open for the (2p3s) Rydberg state. All the observed behavior is mediated by short range DABCO/solvent interactions. In the ensuing discussion we will elaborate the three relaxation pathways proposed for the DABCO/solvent systems studied: solvent enhanced intersystem crossing, electron or charge transfer from DABCO to the solvent, and energy transfer from DABCO to the solvent.

A. Intersystem Crossing. Several observations suggest that intersystem crossing is an important relaxation pathway for the $^1R_1$ (2p3s) Rydberg state of DABCO/rare gas, saturated hydrocarbon, and perfluoro carbon clusters: (1) these clusters have shorter lifetimes than bare DABCO (Table I); (2) the bare molecule formation rate is the same as the cluster $^1R_1$ 0^0 decay rate (see Figure 3); (3) the newly produced bare molecule signal lives for the duration of the experiment (~3.5 μs); (4) the newly produced bare molecule has an ionization energy 564 cm^{-1} larger than the bare molecule $^1R_1$ 0^0 (see Figures 4 and 5); and (5) a strong heavy atom effect on the $^1R_1$ lifetime is observed for these clusters. Solvent induced intersystem crossing gives a consistent picture of these results. Additionally, intersystem crossing is also observed for DABCO/amine and ether solvents as a minor component of the overall $^1R_1$ cluster relaxation.

Note also that since the bare DABCO molecule is generated upon cluster $^1R_1$ 0^0 excitation, ISC must precede IVR and VP. Cluster dissociation occurs on the triplet state potential surface with 564 cm^{-1} of additional cluster van der Waals vibrational energy: following dissociation, which occurs from the cluster state [$^3R_1$ 0^0 DABCO plus 564 cm^{-1} of van der Waals mode excitation],[19] the DABCO molecule is in the $^3R_1$ 0^0 state. This process is most probable based on density of states arguments and results on other systems.[19] The triplet state of DABCO may live for as long as milliseconds under these conditions.

The position of the lowest triplet state of DABCO is fixed at 564 cm^{-1} below the singlet state at 35 222 cm^{-1}. The $^1R_1 - {}^3R_1$ energy separation has been estimated from fluorescence and phosphorescence maxima in solution to be ~2000 cm^{-1}.[7] The Franck–Condon displacements must be different for the two states in solution.

The singlet–triplet energy difference is much smaller for the DABCO (2p3s) Rydberg state than it is for other systems with

(20) Halpern, A. M. *Chem. Phys. Lett.* **1970**, *6*, 296.

Table III. Comparison of the Singlet (2p3s) Excited-State Lifetimes of DABCO/NH_3 and CH_3OCH_3 Clusters as the Function of Cluster Size[a]

DABCO(solvent)$_n$	excitation (cm^{-1})	lifetime (μs)
	NH_3, n =	
1	35 650	0.19
2	35 650	0.25
3	35 650	0.20
	CH_3OCH_3, n =	
1	35 342	0.25
2	35 087	0.057
3	35 087	0.16
4	35 087	0.16
5	35 087	0.15

[a] Ionization energy is 22 222 cm^{-1}.

valence excitations.[21] This small energy gap shows that the Rydberg state 2p and 3s electrons are only weakly correlated.

B. Intermolecular Electron Transfer. The decays of DABCO/amine, ether, and acetonitrile clusters are characterized by a very fast decay of initial intensity plus a constant signal, which must belong to a new state (Figures 7 and 8). A possible assignment of this new state as the DABCO $^3R_1$ (2p3s) Rydberg state is rejected because the cluster in this new state will not dissociate with over 2200 cm^{-1} of added vibrational energy (Figure 10). This cannot be an energy-transfer state because the valence and Rydberg states of the solvent amines and ethers are higher in energy than those of DABCO. The new state cannot be the ground state because the probe energy needed is too small to ionize the ground state. The only plausible alternative is an electron-transfer state

$$[\mathrm{DABCO(X)}_1 \xrightarrow{h\nu} \mathrm{DABCO(X)}_1\ {}^1\mathrm{R}_1 \rightarrow \mathrm{DABCO^+X^-}]$$

The position of this new electron-transfer state can be estimated. A simple expression for the energy of the electron-transfer state relative to the excited $^1R_1$ state is given by[22]

$$E = \mathrm{IE} + \mathrm{EA} + \Delta G \qquad (6)$$

in which IE is the ionization energy of the excited state donor (DABCO $^1R_1$), EA is the electron affinity of the acceptor (solvent), and ΔG is the electrostatic attraction between the positive and negative charges of the transferred state plus the change of all the nonb nded (van der Waals) interactions between the cluster excited and electron transfer states. The ΔG term is large, negative, and has a minimum value. This energy is estimated to be about −3 eV for charge-transfer states.[23] Experimental evidence suggests that EA ~ 0 for these systems:[24] we thus neglect this term. Equation 6 then becomes

$$E = \mathrm{IE(3s)} - 24\ 200\ \mathrm{cm^{-1}} \qquad (7)$$

IE is about 20 000 cm^{-1} (Figure 9) and thus E is −4200 cm^{-1}. The difference between the ionization thresholds of $^1R_1$ (2p3s) and the electron-transfer state is found experimentally to be −650 cm^{-1}. If the potential wells for the electron-transfer (ET) state and the cluster ion are similar and not displaced with respect to one another, then −650 cm^{-1} is the separation between $^1R_1$ and ET. The weakest part of the estimation of the electron-transfer state energy is the value assumed for ΔG.

Nonetheless, the important point here is that for a resonable assumption concerning ΔG, the electron-transfer state lies below the Rydberg state and thus this estimate supports the assignment. The electron-transfer state is important in DABCO/amine, ether, and acetonitrile clusters because the DABCO (2p3s) state has a very low ionization threshold and the (2p3s) state is delocalized.[15]

The primary mechanism for the fast decay of the DABCO/amine, ether, and acetonitrile clusters is the formation of the electron-transfer state. Although intersystem crossing is also available to the (2p3s) singlet Rydberg state, its rate is expected to be similar to that found for saturated hydrocarbons. Thus, $k_{ET}/k_{ISC} \sim 5$.

The decay rate of the initially excited state of DABCO/amines and ethers (ca. (250 ns)$^{-1}$) can be taken approximately to be the electron-transfer rate. This transfer rate is very slow compared to similar processes in other systems.[25] The Rydberg excited state and the electron-transfer state must have a very small coupling, as is suggested by the relatively long lifetime for the $^1R_1$ state.

As shown in Table I, the electron-transfer rate is strongly dependent on cluster geometry. The faster rate is observed for the cluster with the solvent molecule located closer to the nitrogen atom of DABCO (Table I). The coupling between the electron-transfer state and the (2p3s) state must be strongest in this conformation of solute and solvent. This cluster geometry also has the larger bare molecule/cluster red shift of its spectrum.[16]

Table II also makes the point that electron transfer is fastest at the $^1R_1$ 0^0 state of the cluster: excitation of an internal DABCO vibration decreases the electron-transfer rate. This suggests that the electron-transfer process in these clusters is not a simple barrier crossing or a tunneling process. The matrix element for electron transfer must have a significant Franck–Condon factor associated with it. The barrier between the electron transfer and Rydberg states must also be quite large and the electron tunneling coordinate must include a number of nuclear displacements.

C. Energy Transfer. The decay rates for DABCO/benzene, toluene, and CH_3SCH_3 are fast, and no new states can be identified following this process in either the cluster or bare molecule mass channels. Two mechanisms can be suggested to account for this behavior: (1) enhanced internal conversion to the ground state under the influence of the solvent and (2) DABCO/solvent energy transfer through either singlet or triplet states of the coupled solute/solvent system—an off-diagonal electron-transfer (exchange) interaction resulting in energy transfer. We cannot rule out either of these mechanisms. Nonetheless, a study of dimethylethylamine/benzene solutions shows that fluorescence only comes from the benzene component of this solution if the amine is excited: energy transfer between the amine and benzene is suggested to explain this observation.[5,6] The π^* states of benzene and substituted benzenes are below (in absolute energy) the (2p3s) Rydberg state of DABCO. Thus the Rydberg excitation is transferred to the π^* orbitals of the aromatic solvents. Recall that the π states of aromatics are greatly depressed in energy with respect to the 2p states of carbon. This mechanism would populate high-energy $\pi\pi^*$ states of the aromatics which relax to lower states and thus detection of these states is difficult by probe ionization techniques at the energies employed in this effort. Since the interaction is nonresonant and between orbitals of such different shape and extent (3s, σ^*, π^*), the "electron-transfer" interaction referred to in paper 1[16] for this cluster system results in an energy transfer rather than an electron-transfer intermediate state of the DABCO/aromatic solvent clusters.

The exact situation for DABCO/CH_3SCH_3 clusters is less certain because we do not know the energy level structure of methyl sulfide.

V. Conclusions

We have measured the first excited (2p3s) Rydberg state decays for DABCO and its clusters with various solvents by a pump excitation/probe ionization technique. Radiative decay is the major decay mechanism for the (2p3s) Rydberg singlet state of the bare molecule. Three mechanisms appear to be operative for the relaxation of DABCO/solvent clusters. Intersystem crossing

(21) Lipert, R. J.; Colson, S. D.; Sur, A. *J. Phys. Chem.* **1988**, *92*, 183.
(22) Webb, J. D.; Bernstein, E. R. *J. Am. Chem. Soc.* **1978**, *100*, 483.
(23) Person, W. B. *Spectroscopy and Structure of Molecular Complexes*; Yarwood, J., Ed.; Plenum: New York, 1973; p 1.
(24) Jordan, K. D.; Wendoloski, J. J. *J. Chem. Phys.* **1977**, *21*, 145.
(25) Castella, M.; Tramer, A.; Piuzzi, F. *Chem. Phys. Lett.* **1986**, *129*, 105.

dominates for rare gas and saturated hydrocarbon and fluorocarbon solvents. The triplet state of the bare DABCO molecule lies 564 cm^{-1} below the singlet state. Intersystem crossing ($^1R_1 \rightarrow {}^3R_1$) leads to the dissociation of the cluster if the cluster binding energy is smaller than 564 cm^{-1}. The intersystem crossing rate is small but is increased by heavy atoms such as Ar and Kr. This rate depends on cluster geometry: the closer the solvent is to the nitrogen atom of DABCO the larger the intersystem crossing rate. For DABCO clustered with ether and amine solvents, the primary relaxation pathway is internal conversion to an electron-transfer state. The electron-transfer state has a very long lifetime (>3 μs). The electron-transfer rate is determined by the electronic state matrix element and a Franck–Condon factor for the process. We suggest that the reaction coordinate includes a potential barrier and electron tunneling. The transfer rate depends on cluster geometry: the closer the solvent is to the nitrogen atom of DABCO the larger the electron-transfer rate. More solvent molecules do not necessarily enhance the rate. An energy-transfer relaxation pathway, between the (2p3s) Rydberg state of DABCO and the π^* states of the aromatic solvent, is suggested for DABCO/aromatic clusters.

These supersonic jet results suggest that the amine (2p3s) Rydberg excited-state relaxation behavior under the influence of a solvent is a complex process. The conclusions reached in this work probably reflect a general property of Rydberg states: their diffuse orbitals and weakly bound electrons are susceptible to solvent perturbation. Thus the Rydberg states of a molecule are both interactive and reactive.

Acknowledgment. This effort was supported in part by a grant from the U.S. Army Research Office.